Spectral Dependence on the Correction Factor of Erythemal UV for Cloud, Aerosol, Total Ozone, and Surface Properties: A Modeling Study

Sang Seo PARK[1], Yeonjin JUNG[2], and Yun Gon LEE*[3]

[1]*Research Institute for Applied Mechanics, Kyushu University, Fukuoka,* 8160811, *Japan*
[2]*Department of Atmospheric Sciences, Yonsei University, Seoul,* 120749, *South Korea*
[3]*Department of Atmospheric Sciences, Chungnam National University, Daejeon,* 305–764, *South Korea*

(Received 13 September 2015; revised 22 March 2016; accepted 31 March 2016)

ABSTRACT

Radiative transfer model simulations were used to investigate the erythemal ultraviolet (EUV) correction factors by separating the UV-A and UV-B spectral ranges. The correction factor was defined as the ratio of EUV caused by changing the amounts and characteristics of the extinction and scattering materials. The EUV correction factors (CFEUV) for UV-A [CFEUV(A)] and UV-B [CFEUV(B)] were affected by changes in the total ozone, optical depths of aerosol and cloud, and the solar zenith angle. The differences between CFEUV(A) and CFEUV(B) were also estimated as a function of solar zenith angle, the optical depths of aerosol and cloud, and total ozone. The differences between CFEUV(A) and CFEUV(B) ranged from −5.0% to 25.0% for aerosols, and from −9.5% to 2.0% for clouds in all simulations for different solar zenith angles and optical depths of aerosol and cloud. The rate of decline of CFEUV per unit optical depth between UV-A and UV-B differed by up to 20% for the same aerosol and cloud conditions. For total ozone, the variation in CFEUV(A) was negligible compared with that in CFEUV(B) because of the effective spectral range of the ozone absorption band. In addition, the sensitivity of the CFEUVs due to changes in surface conditions (i.e., surface albedo and surface altitude) was also estimated by using the model in this study. For changes in surface albedo, the sensitivity of the CFEUVs was 2.9%–4.1% per 0.1 albedo change, depending on the amount of aerosols or clouds. For changes in surface altitude, the sensitivity of CFEUV(B) was twice that of CFEUV(A), because the Rayleigh optical depth increased significantly at shorter wavelengths.

Key words: Erythemal UV, correction factor, UV-A, UV-B

Citation: Park, S. S., Y. Jung, and Y. G. Lee, 2016: Spectral dependence on the correction factor of erythemal UV for cloud, aerosol, total ozone and surface properties: A modeling study. *Adv. Atmos. Sci.*, **33**(7), 865–874, doi: 10.1007/s00376-016-5201-4.

1. Introduction

Ultraviolet (UV) radiation is spectrally classified into UV-C (100–280 nm), UV-B (280–320 nm) and UV-A (320–400 nm). Most shortwave UV (UV-C and UV-B) is blocked by atmospheric extinction caused by Rayleigh scattering and stratospheric ozone absorption (e.g., Smith et al., 1992; Madronich et al., 1998). The remainder, UV-A and part of UV-B, reaches the surface and affects biological tissue. Although radiation in all UV spectral ranges causes biological damage, the effects are different for respective wavelengths. Several previous studies investigated erythema UV (EUV), which the effects in terms of biological damage have been spectrally considered (e.g., Setlow, 1974; Caldwell et al., 1998; Madronich et al., 1998). In addition, McKinlay and Diffey (1987) defined combined spectral weighting functions pertaining to UV-A and UV-B in the context of erythema occurrence on skin. Because of the biological importance of EUV, a global network of EUV observation stations has been established by several organizations (e.g., the World Ozone and UV Data Center). Instruments designed for broadband observation (Seckmeyer et al., 2010a) as well as hyperspectral observation, which refers to spectral sampling at the sub-nanometer scale, are recommended for EUV observations (Seckmeyer et al., 2010b). It is also recommended that, in addition to EUV observations, monitoring sites also measure total ozone, cloud amounts, and aerosol extinction, which all affect the total EUV extinction. By using a combination of observations and model simulations, the long-term trend and variations of EUV radiation have been studied with consideration of cloud, total ozone, and aerosol (e.g., Casale et al., 2000; Kaurola et al., 2000; Fioletov et al., 2001; den Outer et al., 2005; McKenzie et al., 2011).

The intensity of EUV attenuation caused by respective extinction species is defined by the correction factors (or modification factors) used to adjust EUV estimations under specific conditions to their corresponding EUV values under

* Corresponding author: Yun Gon LEE
Email: yungonlee@gmail.com

reference conditions. Regarding the effects of ozone, McKenzie et al. (1991) reported that a 1% change in total ozone corresponds to a 1.25% change in UV dose. In addition, Kim et al. (2013) showed that the intensity of EUV radiation increases by 1.18% when the total ozone amount decreases by 1%. Related to EUV attenuation by aerosols and clouds, Calbó et al. (2005) identified the effect of cloud on EUV radiation by defining a cloud modification factor (CMF). Burrows (1997) suggested that EUV reductions of 30%–50% and 20%–30% occurred, respectively, near fire source regions and at greater distances from fire sources, compared to the EUV under aerosol-free conditions. Kim et al. (2013) also revealed that the radiation amplification factor of EUV for the aerosol optical depth (AOD) at 320.1 nm is 0.82 under clear sky conditions. To summarize, it is necessary to analyze the factors of influence (i.e., total ozone, cloud, and aerosol) on the variation of surface EUV radiation, and furthermore estimate their correction factors to predict and validate the true EUV radiation on the ground (e.g., Lee et al., 2008; Antón et al., 2009; Bilbao et al., 2014).

Park et al. (2015) considered the additional irradiance in UV-A for UV-index estimation in order to correct spectral limitations of EUV broadband instruments, which only observe in UV-B. In this case, the correction factor for EUV attenuation is to be considered by dividing the two UV regions, UV-A and UV-B. The EUV attenuation associated with different extinction materials, i.e., cloud, aerosol, and ozone, exhibits spectral dependences because of the optical characteristics of the materials themselves. For example, the EUV variation in UV-B is strongly dependent on the intensity of ozone absorption (cf. Smith et al., 1992; Madronich et al., 1998), whereas cloud exhibits weaker spectral sensitivity to whole EUV extinction. Therefore, correction factors for EUV attenuations, such as the modification or amplification factors defined in previous studies, potentially also have a spectral dependence. In addition, the EUV attenuation intensities for specific materials change in complicated cases, such as when the attenuation is caused by several extinction materials and surface conditions, simultaneously (Nichol et al., 2003). Therefore, it is necessary to define each of the correction factors in UV-A and UV-B for accurate EUV estimation.

In this study, simulations of EUV radiation based on a radiative transfer model (RTM) were performed to both identify the spectral dependence of the atmospheric extinction, and separately estimate the respective correction factors for the extinction species in the UV-A and UV-B ranges.

2. Method

In this study, we define an EUV correction factor (CFEUV) that identifies the irradiance differences in EUV caused by changing the amounts and characteristics of the extinction and scattering materials:

$$\mathrm{CFEUV}(\Theta,\tau_a,\tau_c,\Omega,\alpha)=\mathrm{EUV}_{\mathrm{Case}}(\Theta,\tau_a,\tau_c,\Omega,\alpha)/\mathrm{EUV}_{\mathrm{ref}}(\Theta), \quad (1)$$

where $\mathrm{EUV}_{\mathrm{Case}}(\Theta,\tau_a,\tau_c,\Omega,\alpha)$ is the EUV irradiance at the solar zenith angle (SZA), Θ, under specific conditions in the AOD of τ_a, cloud optical depth of τ_c, total ozone amount of Ω, and surface albedo of α. $\mathrm{EUV}_{\mathrm{ref}}(\Theta)$ is the EUV irradiance at the SZA, Θ, under the reference conditions; the total ozone amount (TO3) of 325 DU, surface albedo of 0.1, and surface altitude of 0.0 km with aerosol and cloud-free conditions. For example, the EUV correction factor for cloud was calculated by the ratio of EUV with a constant increment of cloud optical depth (COD) to EUV with COD = 0. Other variables (i.e., total ozone, aerosol, surface albedo, and surface altitude) were assumed to be fixed control variables. Because the SZA value is accurately known at any given time, identical SZA values were applied for both the reference and specific conditions to calculate CFEUV. As a result, the CFEUV definition was determined solely from the intensity difference caused by the atmospheric and surface conditions. In this study, the EUV was divided into two spectral ranges: 280–320 nm for UV-B and 320–400 nm for UV-A. Therefore, we also estimated two different values for the CFEUV; namely, CFEUV(A) and CFEUV(B), which pertain to the UV-A and UV-B spectral ranges, respectively.

To calculate the CFEUV(A) and CFEUV(B) values from the simulations, the simulated irradiance was calculated using the RTM, "UVSPEC", which is contained in the radiation model package, libRadtran (e.g., Mayer et al., 1997; Mayer and Kylling, 2005). Because this model produces fast and accurate irradiance calculations in the UV and visible spectral ranges, it is suitable for calculations regarding EUV and spectral UV. The spectral range used for the calculations was 250 to 400 nm, which covers the EUV spectral range of 280–400 nm. In addition, the model enables the calculation of the monochromatic spectral irradiance in steps of 0.1 nm, which will minimize spectral sampling errors. To calculate Rayleigh scattering by air molecules and consider the temperature variations associated with gas extinction cross sections, a reference dataset containing vertical profiles of the temperature, pressure, and molecular densities of atmospheric gases was used; specifically, the U.S. standard profile (Anderson et al., 1986).

To explore the effects of different atmospheric conditions, simulations were performed to calculate radiation by changing the SZA and TO3, which we used as proxies of changes in the geometry and UV absorption by atmospheric gases, respectively. Figure 1 shows a representative vertical distribution of ozone for the RTM calculation. Although the TO3 value changes as an input parameter of the simulation, the normalized vertical profile of ozone is fixed, as shown in Fig. 1. In order to examine the extinction properties of aerosol and cloud, the AOD and COD were investigated as important parameters in the context of EUV variations. Because the optical depth value has a spectral dependence, we adopted a reference wavelength of 550 nm for both optical depth values. Furthermore, the basic physical properties of aerosol were assumed from Shettle (1989), and these values were basically used as aerosol physical properties in UVSPEC (Mayer and Kylling, 2005). For cloud, the cloud particle was assumed

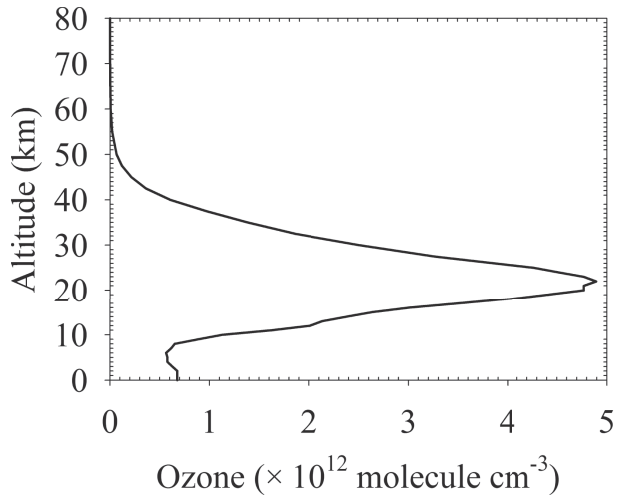

Fig. 1. Vertical distribution of total ozone for the RTM simulation.

Table 1. Input parameters of aerosol and cloud for UV simulation.

Fixed parameters for aerosol/cloud properties	
Single Scattering Albedo (Aerosol)	0.85
Aerosol Asymmetry Factor	0.7
Cloud Asymmetry Factor	0.9
Variable parameters for aerosol/cloud properties	
AOD at 550 nm	0.0–5.0 [Interval = 0.2]
COD at 550 nm	0.0, 0.5, 1.0, 2.0, 3.0, 4.0, 5.0, 6.0, 7.0, 8.5, 10.0, 15.0, 20.0, 30.0

to be a liquid water droplet with effective radius of 10.0 μm. To estimate the spectral dependence of CFEUVs due to AOD and COD, the single scattering albedo (SSA) and the asymmetry factors of both aerosol (g_{aer}) and cloud (g_{cld}) were fixed as shown in Table 1. While the SSA and asymmetry factors are also influential in the process of absorbing and scattering UV radiation, the spectral dependences due to AOD and COD in two UV bands are the focus in this study. For the vertical distribution of aerosol, we assumed that the altitude of the top aerosol layer was 2 km with homogeneous concentration, and the cloud vertical distribution was assumed to be a single layer at an altitude of 4 km with a thickness of 1 km.

In terms of the surface conditions, the surface altitude and its albedo were considered in this study, as these aspects are also among the major factors affecting the EUV and UV spectral irradiance caused by changes in the intensity of Rayleigh scattering at the surface. To explore various surface conditions, we considered surface albedos from 0.0 to 0.5 in intervals of 0.05, as well as surface altitudes from 0.0 to 4.0 km in steps of 1 km. Although the inclination angle of the surface affects the incidence of radiation onto a unit surface area by the reflection angle of the radiation, we only considered horizontal flat surfaces.

3. Results

3.1. *Spectral dependence of the CFEUVs*

Figure 2 shows CFEUV(A) and CFEUV(B) as a function of AOD and COD, assuming 325 DU for TO3, 40° for the SZA, and 0.10 for the surface albedo at sea level. From Fig. 2a, it is clear that both CFEUVs decrease continuously as the AOD increases because of the extinction for direct solar radiation. For AOD = 1.0, CFEUV(A) and CFEUV(B) are estimated at 0.607 and 0.583, respectively, which means that the rate of decline of CFEUV with respect to the AOD ($dCF/d\tau$) is larger for UV-B [$dCF(B)/d\tau$] than for UV-A [$dCF(A)/d\tau$]. For AOD < 1.0, $dCF(B)/d\tau$ is 2%–9% larger than $dCF(A)/d\tau$. However, $dCF(B)/d\tau$ is 1%–20% smaller than $dCF(A)/d\tau$ for AOD > 2.0. This AOD dependence of the rate of decline and the differences between the two spectral ranges are caused by the spectral dependence of the AOD. Because the spectral AOD in the UV-B range is basically larger than that in UV-A, attenuation of the UV irradiance caused by aerosol is more sensitive for UV-B than for UV-A for small AOD. In other words, the AOD threshold of the saturation level for UV

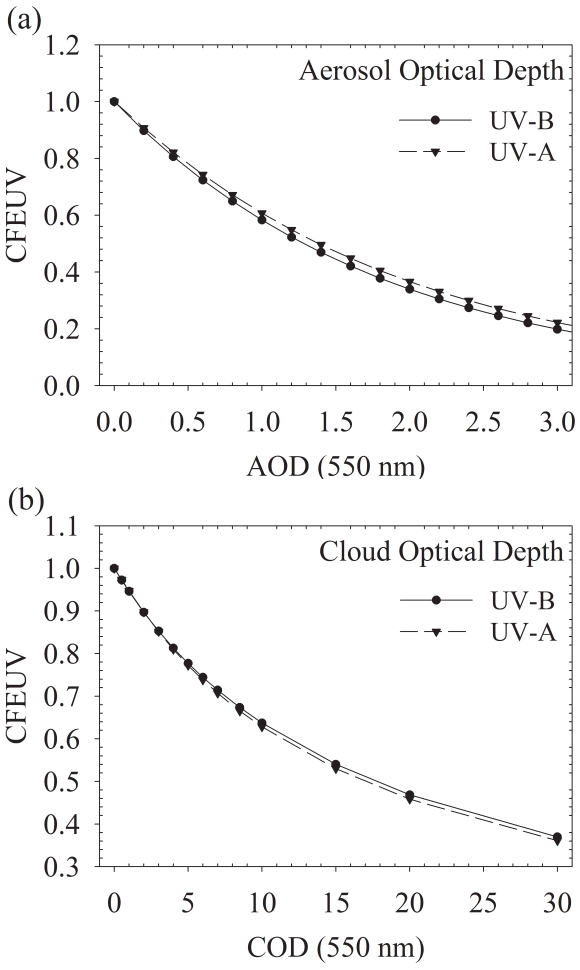

Fig. 2. CFEUV(A) and CFEUV(B) as a function of (a) AOD and (b) COD, with 325 DU for total ozone, 40° for the SZA, and 0.1 for surface albedo at sea surface altitude.

radiation dimming is relatively lower for UV-B than for UV-A. As a result, dCF(B)/dτ is larger for small AOD, but smaller for large AOD, compared with dCF(A)/dτ.

The rate of decline of the CFEUVs for cloud is similar to those for aerosol. However CFEUV(A) is slightly smaller than CFEUV(B) for the same COD, which differs from the aerosol case. Because cloud particle sizes are larger than those for aerosols, the spectral dependence of the COD is weaker than the equivalent dependence of the AOD. For this reason, the spectral dependence of the COD for UV-B is almost the same as that for UV-A, which is opposite to our results for the AOD. However, the effects of Rayleigh scattering are large for UV-B. For this reason, the CFEUV value for UV-B is slightly larger than that for UV-A. For COD = 10.0, CFEUV(B) and CFEUV(A) are 0.637 and 0.628, respectively. In addition, the dCF/dτ value for UV-A and UV-B are almost the same for clouds. This means that the application of a spectrally independent correction factor potentially causes EUV estimation errors of up to a few percent. From this simple analysis, the decrease in UV radiation caused by particles depends on the optical path length, which is a function of both the amount of extinction particles and the observation geometry. For this reason, it is necessary for the analysis of CFEUV to consider SZA information.

Figure 3 and Table 2 show the sensitivity of CFEUV(A) and CFEUV(B) to the AOD and COD as a function of the SZA. The EUV irradiance and its correction factors are sensitive to the observation geometries, especially the SZA (e.g., Nichol et al., 2003, Lee et al., 2015). The reference conditions for the CFEUV calculation were 325 DU for TO3, 0.1 for the surface albedo, and sea level for each value of the SZA. Because the optical path length for direct radiation becomes longer according to the SZA increases, the rates of decline of the CFEUVs per unit AOD and COD increase as the SZA increases. However, the CFEUVs reverse from a decreasing to an increasing trend for SZAs between 60° and 80° in all cases, except for low AODs and CODs. A major reason for this CFEUV reduction is the extinction of the downward direct intensity caused by atmospheric scattering. However, direct radiation at large SZAs is weak because of the long optical path length with large Rayleigh scattering in clear-sky cases. Although the absolute intensity of the UV radiation is reduced when the SZA increases, the CFEUVs increase for large SZAs, in particular because of the small contribution from direct radiation with diffuse radiation dominance.

Figure 4 shows a contour plot of the CFEUV differences between UV-A and UV-B [CFEUV(A/B)] as a function of the SZA. CFEUV(A/B) is defined as

$$\mathrm{CFEUV(A/B)} = [\mathrm{CFEUV(A)} - \mathrm{CFEUV(B)}]/\mathrm{CFEUV(B)}\,, \quad (2)$$

which highlights the spectral sensitivity of the CFEUV under atmospheric conditions. Because the spectral dependence of the AOD is stronger than that of the COD, most cases show positive values for CFEUV(A/B) in the aerosol simulations, except for large SZAs and small AODs. On the other hand, negative CFEUV(A/B) values are estimated for SZA > 40° in the cloud simulations. The values of CFEUV(A/B) tend to be negative because of the large optical path length, but the spectral dependence of the atmospheric optical depth causes a positive value of CFEUV(A/B). These two opposite effects make the final value of the CFEUV different between UV-A and UV-B. From Fig. 4, CFEUV(A/B) is seen to range from −5.0% to 25.0% in the aerosol simulations, and from −9.5% to 2.0% in the cloud simulations. In addition, CFEUV(A/B) decreases as the SZA increases.

Because of changes in the optical path length, the correction factor is sensitive to the SZA and the TO3. Figure 5 shows the sensitivity of CFEUV(A) and CFEUV(B) for TO3 and AOD in the case for a surface albedo of 0.1 and

Table 2. The CFEUV(A) and CFEUV(B) at respective SZAs under total ozone of 325 DU and surface albedo of 0.1 with changing (a) AOD, and (b) COD.

(a) AOD

	AOD = 0.4		AOD = 1.0		AOD = 3.0	
SZA	CFEUV(A)	CFEUV(B)	CFEUV(A)	CFEUV(B)	CFEUV(A)	CFEUV(B)
0	0.858	0.840	0.671	0.638	0.269	0.234
20	0.850	0.832	0.655	0.624	0.255	0.223
40	0.821	0.806	0.607	0.583	0.222	0.199
60	0.768	0.769	0.539	0.539	0.191	0.181
80	0.755	0.794	0.543	0.571	0.198	0.197

(b) COD

	COD = 5.0		COD = 10.0		COD = 20.0	
SZA	CFEUV(A)	CFEUV(B)	CFEUV(A)	CFEUV(B)	CFEUV(A)	CFEUV(B)
0	0.825	0.809	0.679	0.665	0.496	0.488
20	0.811	0.800	0.665	0.657	0.486	0.483
40	0.772	0.777	0.628	0.637	0.458	0.469
60	0.720	0.756	0.584	0.621	0.426	0.458
80	0.725	0.773	0.588	0.636	0.429	0.469

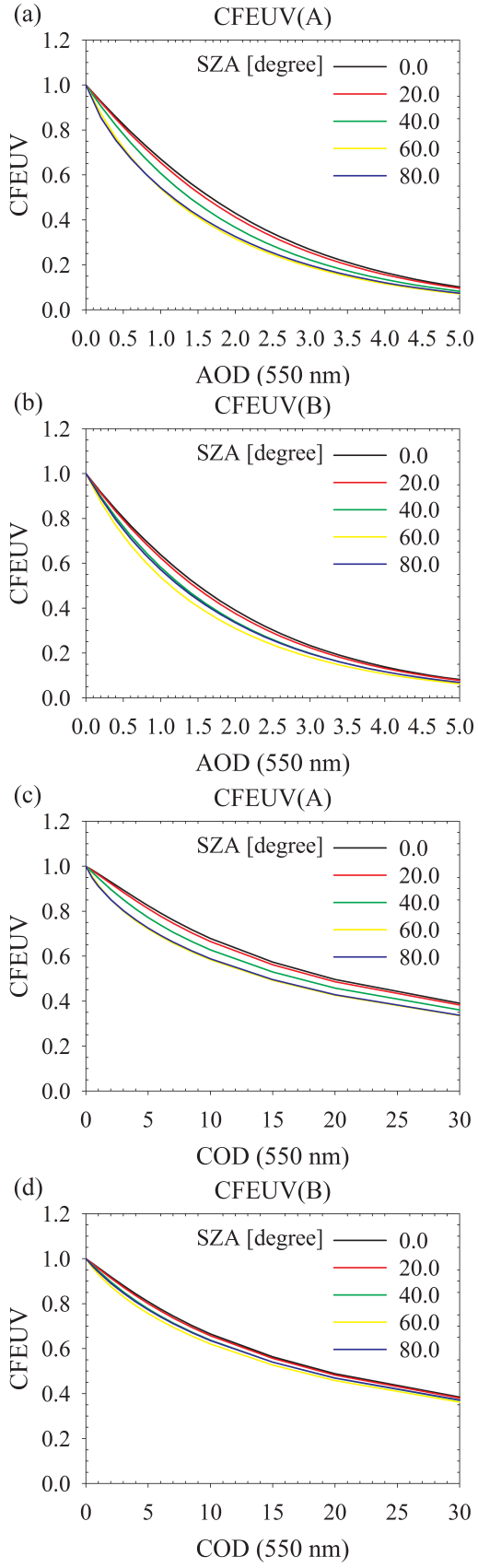

Fig. 3. SZA dependence of (a) CFEUV(A) and (b) CFEUV(B) as a function of AOD, and the dependence of (c) CFEUV(A) and (d) CFEUV(B) as a function of COD.

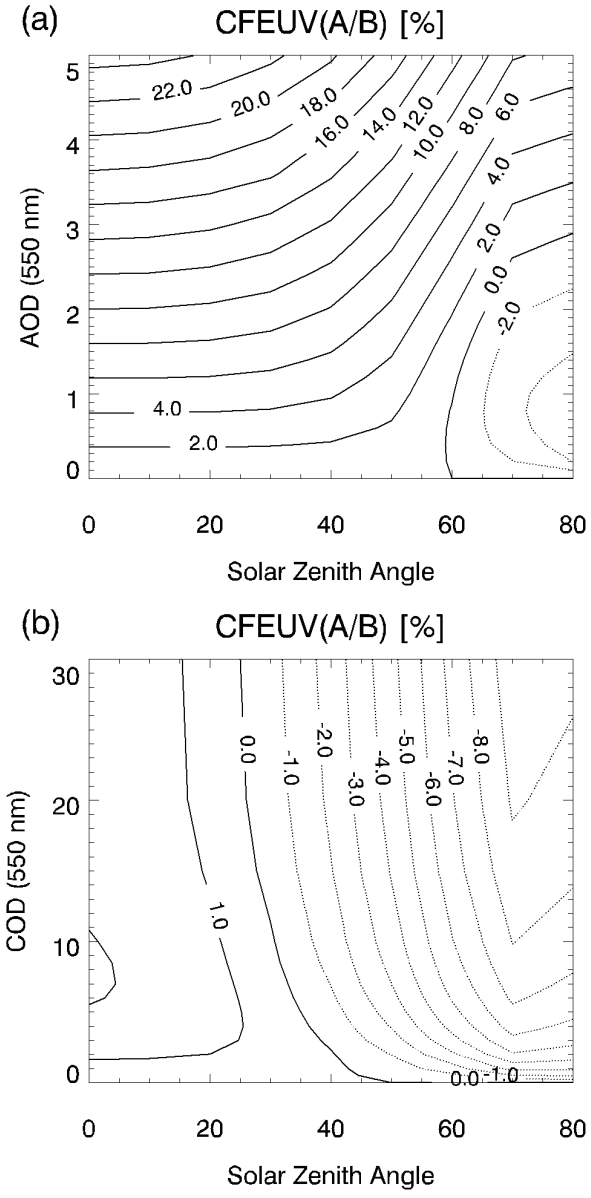

Fig. 4. Relative difference of CFEUV(A) and (B) [CFEUV(A/B)] for (a) SZA and AOD dependence and (b) for SZA and COD dependence.

SZA of 40°. The strong ozone absorption band, the Hartley band, in the wavelength range of 280 to 320 nm, results in CFEUV(B) depending predominantly on the TO3. The rate of decline of CFEUV(B) per unit TO3 [dCF(B)/dTO3] is 0.019–0.069 per 10 DU for AOD = 0.0, and 0.011–0.040 per 10 DU in AOD = 1.0. This range of rates of decline means that 1%–7% of UV-B would change if the TO3 varies by 10 DU. Although the absolute value of dCF(B)/dTO3 decreases as the AOD increases, the relative variation of CFEUV(B) as a function of the TO3 (for values between 250 and 500 DU) is approximately 48% for all AODs. However, the rate of decline of CFEUV(A) per unit TO3 [dCF(A)/dTO3] is 0.001–0.002 per 10 DU, which is 10 times smaller than dCF(B)/dTO3. Although ozone absorption in the Huggins

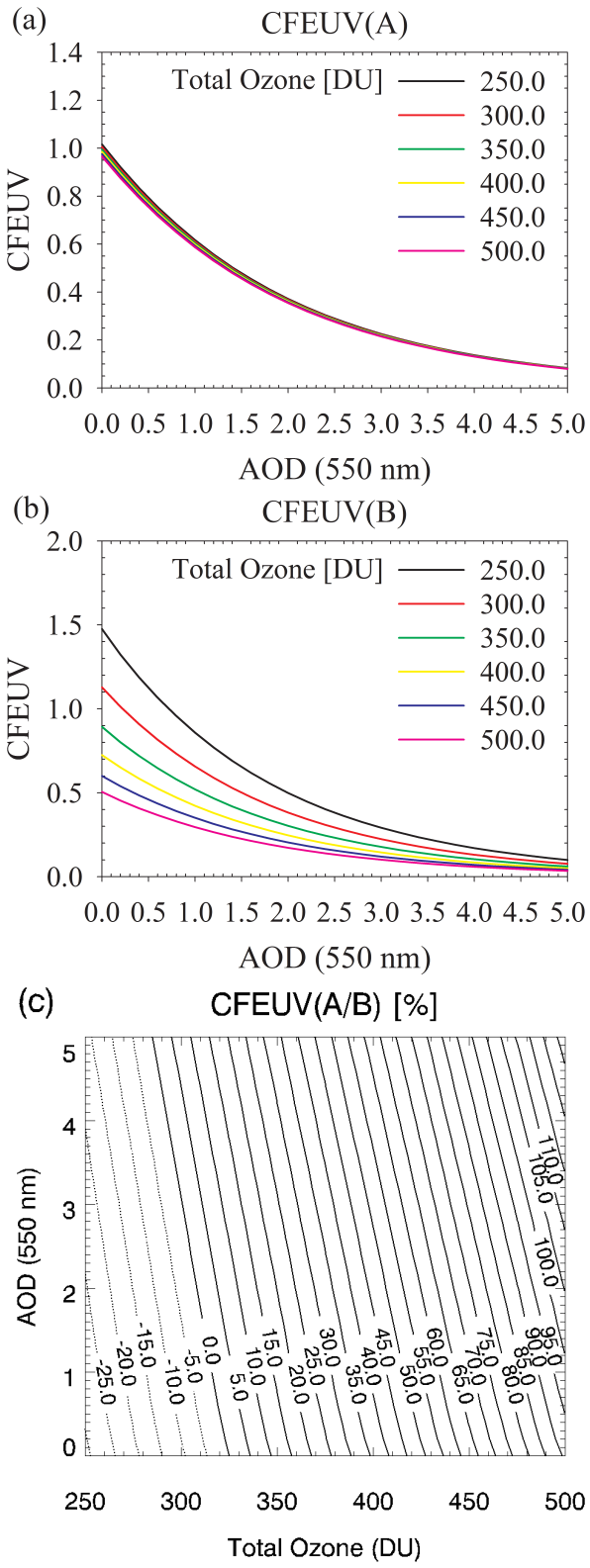

Fig. 5. Sensitivity of (a) CFEUV(A) and (b) CFEUV(B) as a function of total ozone and AOD, and (c) CFEUV(A/B).

band partially overlaps with the UV-A wavelength range, the cross section of the Huggins band in the UV-A is in the order of 1.0×10^{-21} cm^{-2} molecules^{-1}, which results in negligible absorption compared with that in the UV-B range (e.g., Molina and Molina, 1986). Because the relative difference in CFEUV(A) for the TO3 variation from 250 to 500 DU is only about 2%, CFEUV(A) can be assumed to be insensitive to variations in the TO3. The characteristics of the ozone absorption cross section lead to a strong dependence of CFEUV(A/B) on the TO3, as shown in Fig. 5c.

Figure 5c shows that the contour lines of CFEUV(A/B) run almost parallel to the AOD axis. CFEUV(A/B) changes by 5% if either the TO3 changes by 10 DU or the AOD changes by 0.7–1.5. This result means that the spectral dependence of the TO3 for variations of 10 DU is equivalent to that seen for changes of 0.7–1.5 in AOD. However, the CFEUV(A/B) value is mostly dependent on the TO3 value, because the TO3 mostly absorbed UV-B before arriving at the aerosol layer in the troposphere.

Figure 6 shows the sensitivity of CFEUV(B) and CFEUV(A) to the TO3 and the COD under the same conditions as those in Fig. 5. For cloud-free conditions, the dCF(B)/dTO3 is 0.019–0.069 per 10 DU, which is the same value as for AOD = 0.0. For cloudy conditions, dCF(B)/dTO3 ranges from 0.012 to 0.045 per 10 DU for COD = 10.0, which is a similar range as for AOD = 1.0 in Fig. 5. Similarly, the range for dCF(A)/dTO3 is also the same as for the AOD sensitivity in Fig. 5. From these sensitivity results, the conditions between AOD = 1.0 and COD = 10.0 lead to almost the same effect in terms of the spectral sensitivity of CFEUV(B) on the TO3. Because the rate of forward scattering for clouds is higher than the equivalent rate for aerosols, the sensitivity of the CFEUVs to the TO3 value is the same for large COD and small AOD. Figure 6c shows the same contour plot as Figure 5c, but for the COD. Compared with the results for aerosol in Fig. 5c, the contours in Fig. 6c run more closely parallel to the COD axis than those in Fig. 5c. Because cloud particles are larger than aerosol particles, the spectral dependence of the optical depth for clouds is smaller than the dependence for aerosols. Therefore, the sensitivity of CFEUV(A/B) to clouds is much smaller than that to aerosols.

The sensitivity study of CFEUV shows similar results to the results from previous studies. Bilbao et al. (2014) carried out an investigation of EUV irradiance attenuation on Malta in the central Mediterranean Sea. It was found that total ozone reduced EUV irradiance levels in the range of −0.24% to −0.33% DU^{-1}, and AOD at 550 nm reduced EUV irradiance from −28% to 50% per unit AOD (Bilbao et al., 2014). Furthermore, Mateos et al. (2010) observed that cloudy overcast and high solar elevation conditions present a high attenuation of EUV by the interaction between the diffuse component and atmospheric components, like ozone.

3.2. *Correction factor variation as a function of surface properties*

Table 3 shows the variations in the CFEUVs as a function of surface albedo for SZA = 40° and TO3 = 325 DU in clear-sky conditions. It was assumed that the surface albedo was spectrally independent in this simulation. From Table 3, it follows that the EUV intensity increases by 4%–5% if

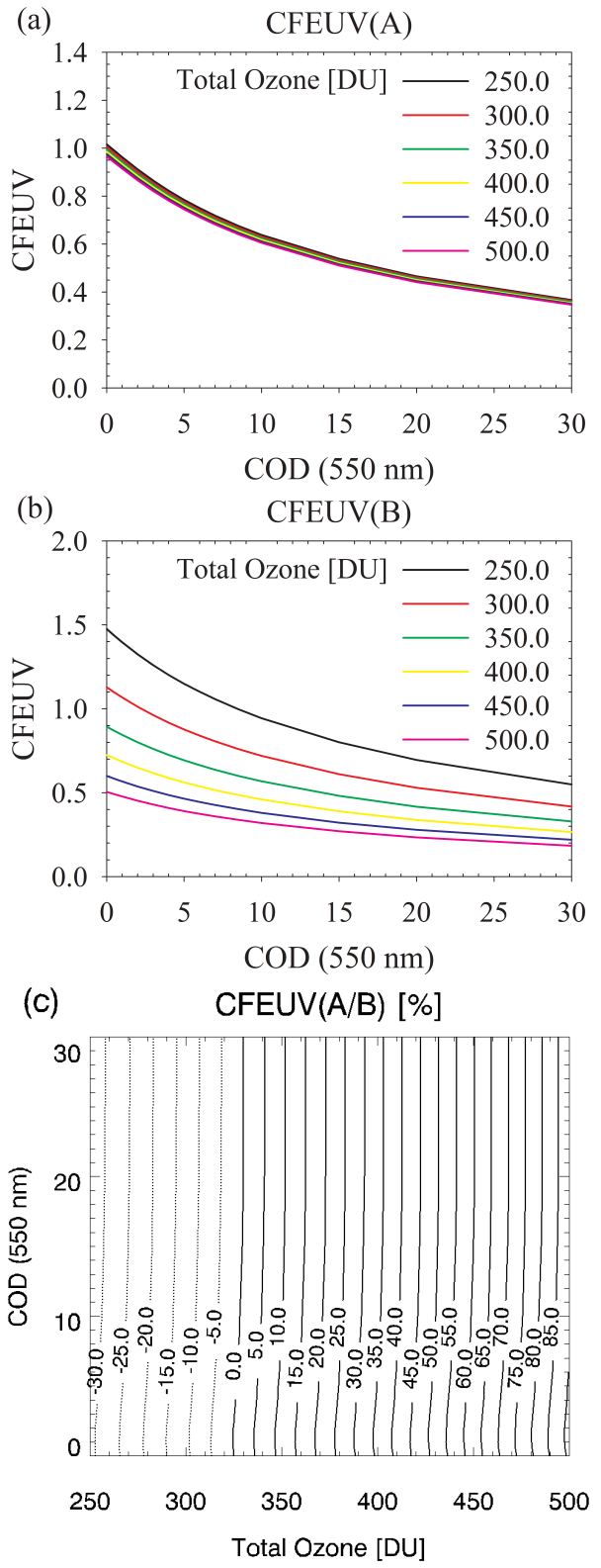

Fig. 6. Sensitivity of (a) CFEUV(A) and (b) CFEUV(B) as a function of total ozone and COD, and (c) CFEUV(A/B).

the surface albedo is changed by 0.1, and these rates of increase of the CFEUVs are enhanced in high surface albedo conditions. This enhancement is caused by the increasing interaction between surface reflection and downward scattering from the atmosphere. CFEUV(A/B) ranges from −0.95% (surface albedo = 0.5) to 0.21% (surface albedo = 0.0), and CFEUV(A/B) decreases as the surface albedo increases. This means that the rate of increase caused by changes in the surface albedo for UV-B is slightly larger than that for UV-A. A major reason for this CFEUV increase, caused by changes in the surface albedo, is downward scattering from the atmosphere above the surface. The optical depth for Rayleigh scattering has a strong spectral dependence, which is a function of wavelength as λ^4. Due to strong Rayleigh scattering in UV-B, the proportion of downward scattered radiation by reflection from the surface is higher for UV-B than for UV-A.

Table 3. Dependence of CFEUV(A), CFEUV(B) and CFEUV(A/B) on surface albedo, with 325 DU for total ozone, 40° for the SZA, and a cloud and aerosol free atmosphere at sea surface altitude. (Reference surface albedo = 0.1)

Surface Albedo	CFEUV(A)	CFEUV(B)	CFEUV(A/B)
0.0	0.964	0.962	0.21%
0.1	1.000	1.000	0.00%
0.2	1.039	1.041	−0.22%
0.3	1.081	1.086	−0.45%
0.4	1.127	1.134	−0.70%
0.5	1.176	1.188	−0.95%

Table 4 shows the sensitivity of the CFEUVs to the surface albedo. From Table 4a, the sensitivity of the CFEUVs to a surface albedo of 0.1 is estimated at 3.6%–4.1% for AOD = 0.0, whereas it is 2.9%–3.1% for AOD = 5.0. The sensitivity to surface albedo decreases as AOD increases for both CFEUV(A) and CFEUV(B). The sensitivity of the CFEUVs is estimated at 7.0%–9.2% for COD = 30.0, which means an increasing sensitivity with increasing cloud cover, as shown in Table 4b. Because clouds are located in the free atmosphere, cloud cover only affects dimming in the context of direct radiation. However, multiple scattering near the surface is rarely affected by clouds. Therefore, the surface albedo effects under cloud cases are more important than those under aerosol cases. However, the aerosol layer is homogeneously located below an altitude of 2 km, as explained in section 2. Because aerosols exist near the surface, they affect both the dimming of direct radiation and multiple scattering between the surface and the atmosphere. For this reason, the sensitivity change of the CFEUVs related to changes in the surface albedo shows opposite trends for aerosols and clouds.

Whereas increasing the surface albedo enhances the UV irradiance caused by Rayleigh scattering, increasing the surface altitude has the opposite effect. The surface altitude correlates linearly with the surface pressure, i.e., it is also linearly related to the intensity of the Rayleigh scattering. By changing the surface altitude from 0 km to 1 km, the surface pressure decreases by 15%, which means that the column integrated air parcel amount changes by about 15%. As a result of decreasing Rayleigh scattering, the UV irradiance at the surface is expected to be enhanced as altitude increases. For this reason, CFEUV(A) and CFEUV(B) are always greater

Table 4. Sensitivity of CFEUVs to surface albedo with changing (a) AOD and (b) COD [albedo (a–b): relative difference of CFEUV sensitivity between albedo value a and b].

(a)

AOD	CFEUV(A) [Albedo (0.1–0.0)]	CFEUV(B) [Albedo (0.1–0.0)]	CFEUV(A) [Albedo (0.2–0.1)]	CFEUV(B) [Albedo (0.2–0.1)]
0	3.60%	3.80%	3.88%	4.11%
1	3.19%	3.28%	3.39%	3.52%
2	3.03%	3.03%	3.19%	3.27%
3	2.93%	2.97%	3.11%	3.12%
4	2.88%	2.91%	3.03%	3.08%
5	2.91%	2.92%	3.03%	3.06%

(b)

COD	CFEUV(A) [Albedo (0.1–0.0)]	CFEUV(B) [Albedo (0.1–0.0)]	CFEUV(A) [Albedo (0.2–0.1)]	CFEUV(B) [Albedo (0.2–0.1)]
0	3.60%	3.80%	3.88%	4.11%
1	4.00%	4.07%	4.36%	4.44%
5	5.17%	4.92%	5.78%	5.46%
10	6.10%	5.62%	6.93%	6.36%
20	7.16%	6.47%	8.36%	7.43%
30	7.76%	6.97%	9.20%	8.08%

than 1.0, as shown in Fig. 7. An increase in surface altitude by 1 km causes a CFEUV change of approximately 0.03–0.05. Furthermore, the spectral difference effect caused by changes in the surface altitude is stronger than that from the surface albedo changes. The rate of increase of CFEUV(B) is twice that of CFEUV(A), i.e., 0.04 km^{-1} and 0.02 km^{-1} for CFEUV(B) and CFEUV(A), respectively. The effects of changes in the surface altitude are directly related to the intensity of Rayleigh scattering, whereas the surface albedo effect is caused by multiple scattering, which is a secondary effect of Rayleigh scattering. For this reason, the spectral dependence of CFEUVs is much stronger than that for the surface albedo effect.

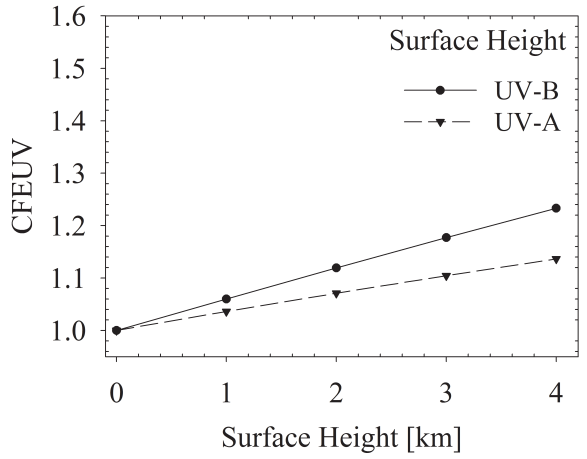

Fig. 7. CFEUV(A) and CFEUV(B) as a function of surface altitude, with 325 DU for total ozone, 40° for the SZA, and a cloud and aerosol free atmosphere at sea surface altitude.

4. Conclusions and discussion

Based on radiative transfer model simulations, this study has estimated the spectral dependence of the EUV correction factors for different atmospheric compositions and surface information. Because of characteristic changes in scattering properties, the sensitivity of CFEUVs to aerosols and clouds shows different trends. CFEUV(A) is larger than CFEUV(B) for most aerosol cases, whereas CFEUV(A) is smaller than CFEUV(B) for most cloud cases. Furthermore, the spectral dependence of the optical characteristics of aerosols and clouds causes differences between CFEUV(A) and CFEUV(B). By considering changes in both the geometry and aerosol or cloud amounts in the simulations, CFEUV(A/B) is found to range from −5.0% to 25.0% for aerosols, and from −9.5% to 2.0% for clouds.

Because a strong ozone absorption band exists in the UV-B region, the characteristic variation in CFEUV(B) is 10 times greater than that in CFEUV(A). dCF(B)/dTO3 is 0.019–0.069 per 10 DU for AOD = 0.0, and 0.011–0.040 per 10 DU for AOD = 1.0. For this reason, 1%–7% of UV-B is affected by the TO3 change of 10 DU. If the TO3 changes from 250 to 500 DU, the CFEUV(B) varies by approximately 48% for all AODs. However, dCF(A)/dTO3 is 0.001–0.002 per 10 DU, which has a negligible effect. The spectral sensitivity of CFEUV(A/B) to the AOD is partially dependent on the TO3, because the TO3 is mostly absorbed in the UV-B range before arriving at the aerosol layer in the troposphere.

For surface conditions, we simulated the dependence on variations in surface albedo and altitude. From the simulations, the sensitivity of the CFEUVs to a surface albedo change of 0.1 was estimated to be 2.9%–4.1%. The sensitivity to changes in the surface albedo decreases as the

AOD increases for both CFEUV(A) and CFEUV(B). However, the sensitivity of the CFEUVs was estimated to be 9.2% at most, for large CODs. The sensitivity difference is mainly caused by differences in the vertical distributions of clouds and aerosols.

Proceeding to the sensitivity to variations in surface altitude, the CFEUVs increase by about 0.03–0.05 km^{-1}. In addition, the rate of increase of CFEUV(B) is twice that of CFEUV(A), i.e., 0.04 km^{-1} and 0.02 km^{-1} for UV-B and UV-A, respectively. As the surface altitude causes changes in surface pressure that affects the intensity of the Rayleigh scattering, the spectral difference between the CFEUVs for different surface altitudes is more significant than that for changes in surface albedo.

Based on this study, it is noted that the spectral dependence of the correction factor could cause potential error in correction factor application, commonly used to estimate or forecast the true EUV from ground-based or model-based clear-sky EUV. Therefore, it will be necessary to perform an error budget study of EUV correction factors by comparing the results with and without consideration of spectral dependences. Furthermore, CFEUVs potentially change with respect to the variations of aerosol and cloud optical properties, scattering phase function, vertical distribution, and spectral SSA. Through further study, it will be necessary to develop a CFEUVs database with detailed consideration.

Acknowledgements. This work was funded by the Korea Meteorological Administration Research and Development Program (Grant No. KMIPA 2015-5170).

REFERENCES

Anderson, G. P., S. A. Clough, F. X. Kneizys, J. H. Chetwynd, and E. P. Shettle, 1986: AFGL atmospheric constituent profiles (0.120km). Tech. Rep. AFGL-TR-86-0110, Air Force Geophysics Lab., Hanscom Air Force Base, Bedford, Mass.

Antón, M., A. Serradno, M. L., Cancillo, and J. A. García, 2009: An empirical model to estimate ultraviolet erythemal transmissivity. *Ann. Geophys.*, **27**, 1387–1398.

Bilbao, J., R. Román, C. Yousif, D. Mateos, and A. de Miguel, 2014: Total ozone column, water vapour and aerosol effects on erythemal and global solar irradiance in Marsaxlokk, Malta. *Atmos. Environ.*, **99**, 508–518.

Burrows, W. R., 1997: CART regression models for predicting UV radiation at the ground in the presence of cloud and other environmental factors. *J. Appl. Meteor.*, **36**(5), 531–544.

Calbó, J., D. Pagès, and J. A. González, 2005: Empirical studies of cloud effects on UV radiation: A review. *Rev. Geophys.*, **43**(2), doi: 10.1029/2004RG000155.

Caldwell, M. M., L. O. Björn, J. F. Bornman, S. D. Flint, G. Kulandaivelu, A. H. Teramura, and M. Tevini, 1998: Effects of increased solar ultraviolet radiation on terrestrial ecosystems. *Journal of Photochemistry and Photobiology B: Biology*, **46**(1-3), 40–52.

Casale, G. R., D. Meloni, S. Miano, S. Palmieri, A. M. Siani, and F. Cappellani, 2000: Solar UV-B irradiance and total ozone in Italy: Fluctuations and trends. *J. Geophys. Res.*, **105**(D4), 4895–4901.

den Outer, P. N., H. Slaper, and R. B. Tax, 2005: UV radiation in the Netherlands: Assessing long-term variability and trends in relation to ozone and clouds. *J. Geophys. Res.*, **110**, D02203, doi: 10.1029/2004JD004824.

Fioletov, V. E., L. J. B. McArthur, J. B. Kerr, and D. I. Wardle, 2001: Long-term variations of UV-B irradiance over Canada estimated from Brewer observations and derived from ozone and pyranometer measurements. *J. Geophys. Res.*, **106**(D19), 23009–23027.

Kaurola, J., P. Taalas, T. Koskela, J. Borkowski, and W. Josefsson, 2000: Long-term variations of UV-B doses at three stations in northern Europe. *J. Geophys. Res.*, **105**(D16), 20813–20820.

Kim, J., H. K. Cho, J. Mok, H. D. Yoo., and N. Cho, 2013: Effects of ozone and aerosol on surface UV radiation variability. *Journal of Photochemistry and Photobiology B: Biology*, **119**, 46–51.

Lee, Y. G., J. Kim, H.-K. Cho, B. C. Choi, J. Kim, S. R. Chung, and I. S. Park, 2008: Forecast of UV-index over Korea with improved total ozone prediction and effects of aerosol, clouds and surface albedo. *Asia-Pacific J. Atmos. Sci.*, **44**(4), 381–400.

Lee, Y. G., J.-H. Koo, and J. Kim, 2015: Influence of cloud fraction and snow cover to the variation of surface UV radiation at King Sejong station, Antarctica. *Atmos. Res.*, **164–165**, 99–109.

Madronich, S., R. L. McKenzie, L. O. Björn, and M. M. Caldwell, 1998: Changes in biologically active ultraviolet radiation reaching the Earth's surface. *Journal of Photochemistry and Photobiology B: Biology*, **46**(1–3), 5–19.

Mateos, D., J. Bilbao, A. de Miguel, and A. Pérez-Burgos, 2010: Dependence of ultraviolet (erythemal and total) radiation and CMF values on total and low cloud covers in Central Spain. *Atmospheric Research*, **98**(1), 21–27.

Mayer, B., and A. Kylling, 2005: Technical note: The libRadtran software package for radiative transfer calculations—description and examples of use. *Atmos. Chem. Phys.*, **5**, 1855–1877.

Mayer, B., G. Seckmeyer, and A. Kylling, 1997: Systematic long-term comparison of spectral UV measurements and UVSPEC modeling results. *J. Geophys. Res.*, **102**(D7), 8755–8767.

McKinlay, A. F., and B. L. Diffey, 1987: A reference action spectrum for ultra-violet induced erythema in human skin. *Human Exposure to Ultraviolet Radiation: Risks and Regulations*, W. F. Passchier and B. F. M. Bosnajakovic, Eds., Elsevier, 83–87.

McKenzie, R. L., W. A. Matthews, and P. V. Johnston, 1991: The relationship between erythemal UV and ozone, derived from spectral irradiance measurements. *Geophys. Res. Lett.*, **18**(12), 2269–2272.

McKenzie, R. L., P. J. Aucamp, A. F. Bais, L. O. Björn, M. Ilyas, and S. Madronich, 2011: Ozone depletion and climate change: impacts on UV radiation. *Photochemical & Photobiological Sciences*, **10**(2), 182–198.

Molina, L. T., and M. J. Molina, 1986: Absolute absorption cross sections of ozone in the 185- to 350-nm wavelength range. *J. Geophys. Res.*, **91**(D13), 14501–14508.

Nichol, S. E., G. Pfister, G. E. Bodeker, R. L. McKenzie, S. W. Wood, and G. Bernhard, 2003: Moderation of cloud reduction of UV in the Antarctic due to high surface albedo. *J. Appl. Meteor.*, **42**, 1174–1183.

Park, S. S., Y. G. Lee, and J. H. Kim, 2015: Impact of UV-A radiation on erythemal UV and UV-index estimation over Korea. *Adv. Atmos. Sci.*, **32**(12), 1639–1646, doi: 10.1007/s00376-

015-4231-7.

Setlow, R. B., 1974: The wavelengths in sunlight effective in producing skin cancer: A theoretical analysis. *Proceedings of the National Academy of Sciences of the United States of America*, **71**(9), 3363–3366.

Shettle, E. P., 1989: Models of aerosols, clouds, and precipitation for atmospheric propagation studies. Paper Presented at Conference on Atmospheric Propagation in the UV, Visible, IR, and MM-Wave Region and Related Systems Aspects, NATO Adv. Group for Aerosp. Res. and Dev., Copenhagen.

Smith, R. C., Z. M. Wan, and K. S. Baker, 1992: Ozone depletion in Antarctica: Modeling its effect on solar UV irradiance under clear-sky conditions. *J. Geophys. Res.*, **97**(C5), 7383–7397.

Seckmeyer, G., A. Bais, G. Bernhard, M. Blumthaler, B. Johnsen, K. Lantz, and R. McKenzie, 2010a: Instruments to measure solar ultraviolet radiation part 3: Multi-channel filter instruments, Technical Report No. 190, WMO/TD-No. 1537, *WMO, Global Atmospheric Watch*, 55 pp.

Seckmeyer, G., A. Bais, M. Blumthaler, S. Drüke, P. Kiedron, K. Lantz, R. McKenzie, and S. Riechelmann, 2010b: Instruments to measure solar ultraviolet radiation part 4: Array Spectraoradiometers, Technical Report No. 191, WMO/TD-No. 1538, *WMO, Global Atmospheric Watch*, 43 pp.